THE ADINI FINITE ELEMENT ON LOCALLY REFINED MESHES

D. GALLISTL

Abstract. This work introduces a locally refined version of the Adini finite element for the planar biharmonic equation on rectangular partitions with at most one hanging node per edge. If global continuity of the discrete functions is enforced, for such method there is some freedom in assigning the normal derivative degree of freedom at the hanging nodes. It is proven that the convergence order h^2 known for regular solutions and regular partitions is lost for any such choice, and that assigning the average of the normal derivatives at the neighbouring regular vertices is the only choice that achieves a superlinear order, namely $h^{3/2}$ on uniformly refined meshes. On adaptive meshes, the method behaves like a first-order scheme. Furthermore, the reliability and efficiency of an explicit residual-based error estimator are shown up to the best approximation of the Hessian by certain piecewise polynomial functions.

1. Introduction and main results

While Galerkin methods enjoy the error bound from Céa's lemma and, therefore, local mesh refinement with nested spaces does not increase the approximation error, in nonconforming discretizations —a popular choice for the biharmonic equation— local refinement of the mesh resolution may potentially disimprove the situation. The main purpose of this work is an analysis of this phenomenon in a model situation. The Adini finite element method (FEM) is one of the earliest methods for numerically solving the biharmonic equation [1, 5]. It is a standard four-noded rectangular element in the engineering literature, and therein also referred to as Adini–Clough–Melosh element [11]. Given a rectangular partition $\mathcal{T}$ of the underlying domain $\Omega \subseteq \mathbb{R}^2$, the shape function space for every rectangle T is the space of cubic polynomials over T enriched by the two monomials x^3y and xy^3, where the Cartesian coordinates of a point in the plane are denoted by x, y and the mesh is assumed to be aligned with the Cartesian axes. The corresponding twelve degrees of freedom are the point evaluation of a function and the evaluation of its first-order partial derivatives in any of the four vertices. The resulting finite element, schematically shown in the mnemonic diagram of Figure 1, is easy to implement and its a priori error analysis is theoretically well understood when regular partitions are used. Regularity of a partition $\mathcal{T}$ means that if any vertex z of an element $T \in \mathcal{T}$ belongs to some element $K \in \mathcal{T}$, it is automatically also a vertex of K. For such regular meshes it is known that the method converges at the order h^2 under uniform mesh refinement if the solution is sufficiently regular, h being the maximal mesh size [5, 10, 9]. In presence of singularities of the solution, the convergence order is significantly reduced and adaptive mesh refinement towards the singularity becomes mandatory, a case not studied so far in the literature on the Adini FEM. On rectangular partitions with bounded aspect ratio, such refinement necessarily

Date: 21st January 2025.
2020 *Mathematics Subject Classification.* 65N12, 65N15, 65N30.
Key words and phrases. nonconforming, hanging node, Kirchhoff plate, serendipity.
Supported by the European Research Council (ERC Starting Grant *DAFNE*, ID 891734).

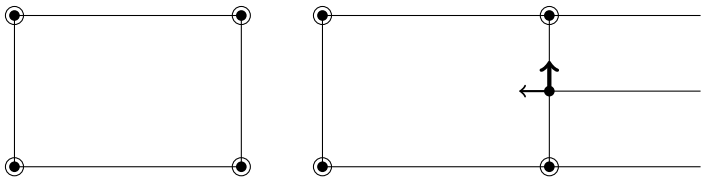

FIGURE 1. Mnemonic diagram of Adini's finite element (left); degrees of freedom at a hanging node (right).

requires elements with irregular vertices (commonly called hanging nodes), i.e., a vertex z of a rectangle T may belong to an edge of another rectangle K without being a vertex of it. The degrees of freedom attached to that hanging node are then subject to some interpolation constraint. The typical situation is displayed in Figure 1. In the case of the Adini element, the value and the derivative in the direction tangential to the edge are prescribed by the condition of the function to be globally continuous. The continuity condition for the partial derivative in the direction normal to the edge, however, is not canonically prescribed because the Adini FEM is a nonconforming method, meaning that the discrete functions are globally continuous but their gradients may be discontinuous so that the discrete functions may possibly not belong to $H^2(\Omega)$, the energy space for the biharmonic equation. Two obvious possibilities (out of many others) are: either the degree of freedom is set in such a way that it interpolates the partial derivative on the neighbouring element; or it is simply chosen as the average of the partial derivatives at the neighbouring vertices determining the edge that contains the irregular vertex z in its interior. It is obvious that the latter choice cannot retain the quadratic approximation order h^2 known from the regular case because the averaging operation does not conserve cubic polynomials. However, in this work it is proven that it is the only possible choice (in the class of linear, local, and coordinate-independent couplings) that yields a superlinear order, namely $h^{3/2}$ on uniform refinements of an initial irregular mesh subject to the condition of Definition 2.1 below.

The design of the Adini element does not involve average integrals of normal derivatives over edges as degrees of freedom, in contrast to nonconforming methods like the Morley element and others [10]. This prevents the element from passing certain patch tests, and the error analysis is more involved and relies on the choice of the shape function space, which is the same as for the lowest-order serendipity element [2]. Consequently, a reliability proof for a residual-based error estimator has not been available [3, 6]. Furthermore, the definition of the element on meshes with hanging nodes is not straightforward because an analogue to [4, condition (A2)] is not satisfied by the normal derivative. As the first main results in this work, it is shown that the quadratic approximation order is necessarily lost in the presence of hanging nodes, showing that best-approximation results in the fashion of [8] are unavailable. It is shown that a suitable assignment of local degrees of freedom at hanging nodes can lead to $h^{3/2}$ convergence.

Theorem A (a priori error estimate)**.** *Let $f \in L^2(\Omega)$ be such that the exact solution u to the biharmonic problem* (2.1) *satisfies $u \in H^4(\Omega) \cap W^{3,\infty}(\Omega)$. Let $(\mathcal{T}_h)_h$ be a sequence of uniform refinements of an initial partition that satisfies the mesh condition of Definition 2.1 and contains at least one irregular vertex. Let $u_h \in V_h$ denote the finite element solution to* (2.2) *where V_h is the Adini finite element space with regular assignment in the sense of Definition 3.1. The averaging assignment, that is the choice of V_h according to* (3.2)*, satisfies*

$$|||u - u_h|||_h \lesssim h^2 \|u\|_{H^4(\Omega)} + h\|u\|_{H^3(\cup \mathcal{T}^{\mathrm{irr}})}$$

where $\cup\mathcal{T}^{\mathrm{irr}}$ *from* (4.1) *is the area covered by elements with irregular vertices. In particular, it satisfies the asymptotic bound*

$$\|\!|u - u_h|\!\|_h \lesssim h^{3/2}(\|u\|_{H^4(\Omega)} + \|u\|_{W^{3,\infty}(\Omega)})$$

on uniformly refined meshes. For any other admissible assignment there exists a right-hand side f *such that the solution* $u \in C^\infty(\overline{\Omega})$ *is smooth, but*

$$\|\!|u - u_h|\!\|_h \gtrsim h.$$

Furthermore, a residual-based a posteriori error estimator is shown to be reliable and efficient up to terms that are second-order accurate on uniform meshes, but only first-order on more general meshes (details on the notation follow in §2).

Theorem B (a posteriori error estimate)**.** *Let* $\mathcal{T}$ *be an 1-irregular partition satisfying the mesh condition of Definition 2.1 and* V_h *be chosen according to the averaging assignment* (3.2)*. The solution* u *to the biharmonic problem* (2.1) *with right-hand side* $f \in L^2(\Omega)$ *and its Adini finite element discretization* u_h *from* (2.2) *satisfy, with* $\boldsymbol{\eta}$*,* $\boldsymbol{\eta}(T)$ *defined in* (5.2)*, the reliability estimate*

$$\|\!|u - u_h|\!\|_h \lesssim \boldsymbol{\eta}$$

and local efficiency

$$\boldsymbol{\eta}(T) \lesssim \|\!|u - u_h|\!\|_{h,\omega_T} + \|(1 - \Pi^{\mathcal{T}})D^2 u\|_T + \|h^2(1 - \Pi_0)f\|_{\omega_T}$$

for any $T \in \mathcal{T}$ *with element patch* ω_T *and the projection* $\Pi^{\mathcal{T}}$ *from* (5.1)*.*

While its efficiency part is not new and can be proven with standard arguments [12], more importantly Theorem B also provides a reliability result of an a posteriori error estimator for the Adini element, which partly proves a conjecture of [3] and explains the results of their numerical experiments. Therein, the error estimator $\boldsymbol{\eta}$ (up to the additional local projection error $\|(1 - \Pi^{\mathcal{T}})D^2 u\|_T$ not considered there) was experimentally observed to be an upper error bound on uniformly refined meshes. Theorem B theoretically justifies the observed convergence rates of the error estimator in [3].

The results presented here allow for two conclusions. The first one is that the Adini FEM can be used a first-order method for resolving corner singularities or non-rectilinear (possibly curved) domains. Since the Adini shape function space is that of the serendipity family [2], the element cannot be mapped to general quadrilaterals like trapeziums without loss of approximation quality, see the discussion in [10]. The local resolution variant of the method proposed here thus makes the Adini FEM more competitive for such situations. In some cases, it even satisfies superlinear convergence. Secondly, and perhaps more fundamentally, the analysis shows that the quadratic convergence order is necessarily lost under fairly reasonable coupling conditions at hanging nodes. This highlights that nonconforming methods do not naturally generalize to irregular partitions in absence of further structural conditions. In particular, local refinement can significantly deteriorate the approximation (as proven in Theorem A and illustrated by numerical results in §6.1), and best-approximation results analogous to those formulated in [8] do not hold in this case.

This article is organized as follows: §2 defines the necessary data structures around finite element meshes and introduces the Adini element. The assignment at hanging nodes is discussed in §3. The proof of Theorem A is provided in §4, while §5 provides the proof of Theorem B. Numerical experiments are shown in §6. Finally, some important but technical estimates for discrete functions are provided in the appendices §A–§D.

Throughout this work, standard notation on Lebesgue and Sobolev spaces is used. The L^2 norm over a measurable set ω is denoted by $\|\cdot\|_\omega$ with the convention $\|\cdot\| = \|\cdot\|_\Omega$. Polynomial functions of total resp. partial degree not greater than k are denoted by P_k resp. Q_k. The notation $a \lesssim b$ or $b \gtrsim a$ indicates an inequality $a \leq Cb$ with a constant independent of the mesh size; $a \approx b$ means $a \lesssim b \lesssim a$.

2. Adini's finite element for the biharmonic equation

Let $\Omega \subseteq \mathbb{R}^2$ be an open and bounded rectilinear Lipschitz polygon. Given a right-hand side $f \in L^2(\Omega)$, the biharmonic problem with clamped boundary conditions seeks $u \in H^2_0(\Omega)$ such that

$$a(u,v) = (f,v)_{L^2(\Omega)} \quad \text{for all } v \in H^2_0(\Omega), \tag{2.1}$$

where the bilinear form a is defined by

$$a(v,w) := \int_\Omega D^2 v : D^2 w \quad \text{for any } v, w \in H^2(\Omega)$$

and the colon : denotes the Frobenius inner product of matrices.

The following notation related to a partition $\mathcal{T}$ of Ω is used. The set of vertices (extremal points) of a rectangle is denoted by $\mathcal{V}(T)$. The set of all vertices of $\mathcal{T}$ is denoted by $\mathcal{V}$. A vertex $z \in \mathcal{V}$ for which $z \in T \in \mathcal{T}$ implies $z \in \mathcal{V}(T)$, i.e., z is one of the four vertices of T, is called a regular vertex, and the set of such vertices is denoted by $\mathcal{V}^{\mathrm{reg}}$. The remaining irregular vertices are denoted by $\mathcal{V}^{\mathrm{irr}} = \mathcal{V} \setminus \mathcal{V}^{\mathrm{reg}}$. Throughout this work, the notions *hanging node* and *irregular vertex* are used interchangeably. Any irregular $z \in \mathcal{V}^{\mathrm{irr}}$ necessarily lies on the interior of an edge E of some rectangle T that is the convex combination of two vertices $z_1, z_2 \in \mathcal{V}(T)$, called the neighbouring vertices. In particular $z \in E = \mathrm{conv}\{z_1, z_2\}$. Throughout this paper, we work on classes of partitions with uniformly bounded aspect ratio. The L^2 projection to piecewise (possibly discontinuous) P_k functions is denoted by Π_k. For $z \in \mathcal{V}$ and $T \in \mathcal{T}$ we define the usual patches

$$\omega_z := \mathrm{int}(\cup\{K \in \mathcal{T} : z \in K\}) \quad \text{and} \quad \omega_T := \cup\{\omega_z : z \in \mathcal{V}(T)\}.$$

The outer unit normal of the boundary of a rectangle T is denoted by n_T. The set of all edges is denoted by $\mathcal{E}$. Every edge has a (globally fixed) normal vector n_E and a tangential vector t_E. If the meaning is clear from the context and there is no risk of confusion, the symbols n and t are sometimes used without index in expressions like ∂^2_{nn}, ∂^2_{nt}, etc. The diameter of a rectangle T and an edge E are denoted by h_T and h_E, respectively. The piecewise constant mesh-size function h is defined by $h|_T := h_T$ for any $T \in \mathcal{T}$. If the letter h is used in global expressions like $O(h^s)$ or outside norms, it denotes the maximum of the mesh size function.

The piecewise Hessian with respect to $\mathcal{T}$ is denoted by D^2_h, and the index h is also used to indicate piecewise partial derivatives $\partial_{j,h}$ of piecewise smooth functions. Any rectangle $T \subseteq \mathbb{R}^2$ will be assumed to be aligned with the Cartesian axes, so that any of its faces is parallel to either the x or y axis. The shape function space $\mathcal{A}$ is that of cubic polynomials enriched by the two elements xy^3 and x^3y, written

$$\mathcal{A} = P_3 + \langle xy^3, x^3y \rangle$$

where angle brackets denote the linear hull. If there is no risk of confusion, a polynomial function will not be distinguished from its restriction to or its extension from some subdomain of $\mathbb{R}^2$ throughout this work. Given a rectangle T, the twelve degrees of freedom of the Adini finite element are the point evaluations of a function and of its first partial derivatives in those vertices. A corresponding diagram is displayed in Figure 1. Given Ω, let $\mathcal{T}$ be a finite partition into rectangles such that

the elements of T cover the domain $\cup_{T\in\mathcal{T}}T=\overline{\Omega}$ and the intersection of the interior of any two distinct elements is empty. The space of piecewise Adini functions reads

$$\mathcal{A}(\mathcal{T}):=\{v\in L^\infty(\Omega):v|_T\in\mathcal{A}\text{ for any }T\in\mathcal{T}\}.$$

If $\mathcal{T}$ is any such partition (with or without hanging nodes), the global finite element space with clamped boundary condition and gradient continuity at the regular vertices reads

$$\widehat{V}_h:=C(\overline{\Omega})\cap\left\{v\in\mathcal{A}(\mathcal{T})\,\middle|\,\begin{array}{r}\nabla v\text{ is continuous in the interior regular vertices of }\mathcal{T}\\ v\text{ and }\nabla v\text{ vanish on the boundary vertices of }\mathcal{T}\end{array}\right\}.$$

The continuity requirement shows that $\widehat{V}_h$ is spanned by $\mathcal{A}(\mathcal{T})$ functions that are continuous in all vertices, with continuous gradient in all regular vertices and with continuous tangential derivative at irregular vertices ('tangential' referring to the edge containing the hanging node). No condition is made on the normal derivative at such vertex although it is a local degree of freedom for the finite element. For regular partitions, $V_h=\widehat{V}_h$ is the standard Adini finite element space known from the literature. In this case it is known that $V_h\subseteq C(\overline{\Omega})$ is a space of continuous functions with possibly discontinuous piecewise derivatives. This means that V_h is a subspace of the Sobolev space $H^1_0(\Omega)$ but in general not a subspace of the energy space $H^2_0(\Omega)$ for the biharmonic problem, whence it is referred to as nonconforming. If the partition contains irregular vertices, a subspace $V_h\subseteq\widehat{V}_h$ needs to be considered such that the discrete problem is well posed. The Adini finite element discretization is based on the discrete bilinear form

$$a_h(v,w):=\int_\Omega D_h^2v:D_h^2w\quad\text{for any }v,w\in H^2_0(\Omega)+\widehat{V}_h$$

where D_h^2 denotes the piecewise Hessian with respect to $\mathcal{T}$. Under the admissibility condition of Definition 3.1 below, V_h is such that a_h is positive definite over V_h. The seminorm induced by a_h and denoted by $|\!|\!|\cdot|\!|\!|_h$ is a norm on V_h under this assumption. The discretization seeks $u_h\in V_h$ such that

$$a_h(u_h,v_h)=(f,v_h)_{L^2(\Omega)}\quad\text{for all }v_h\in V_h. \tag{2.2}$$

It is well known that, for regular partitions, this is a convergent method on a sequence of uniformly refined rectangles with maximal mesh size h. The error bound shown in [9] states the quadratic order

$$|\!|\!|u-u_h|\!|\!|_h\lesssim h^2\|u\|_{H^4(\Omega)}.$$

In the general case of possibly nonconvex domains, the assumed regularity is unrealistic, and local mesh refinement is required for resolving singularities or the domain geometry. For rectangular and shape-regular partitions, this necessarily leads to hanging nodes. The main question is which continuity properties to enforce at hanging nodes in the definition of V_h in order to obtain a method with good convergence properties. Here, we focus on 1-irregular partitions with a maximum of one hanging node per edge.

Definition 2.1 (mesh condition)**.** We say that $\mathcal{T}$ satisfies the mesh condition if for any irregular $z\in\mathcal{V}^{\mathrm{irr}}$ (1) its neighbouring vertices z_1,z_2 are regular; (2) z is the midpoint of $\mathrm{conv}\{z_1,z_2\}$; (3) any pair $z_1,z_2\in\mathcal{V}^{\mathrm{reg}}$ of regular vertices hosts at most one irregular vertex, i.e., $\mathrm{card}(\mathrm{conv}\{z_1,z_2\}\cap\mathcal{V}^{\mathrm{irr}})\le 1$.

This condition means that every edge contains at most one hanging node, which is necessarily the midpoint; and that any edge with a hanging node connects two regular vertices. Figure 2 shows some configurations excluded by this condition. Let $\mathcal{T}$ be a partition satisfying the condition of Definition 2.1. Such partitions allow for simple Q_1 interpolation. For any function v over $\overline{\Omega}$ that is continuous in the regular

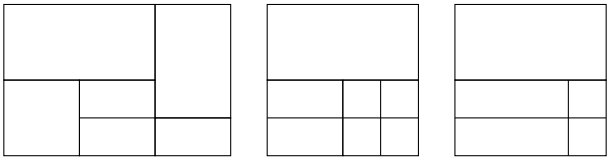

FIGURE 2. Mesh configurations excluded by Definition 2.1. Left: some neighbouring vertices are irregular. Middle: an edge contains more than one irregular vertex. Right: the irregular vertex is not the midpoint of an edge.

vertices $\mathcal{V}^{\mathrm{reg}}$, the interpolation Qv is the globally continuous and piecewise bilinear function defined by assigning the nodal value of v at the regular vertices and, for irregular vertices, the average of the values at the two neighbouring vertices. That is, Qw is defined by

$$Qv(z) = \begin{cases} w(z) & \text{if } z \in \mathcal{V}^{\mathrm{reg}} \\ 2^{-1}(w(z_1) + w(z_2)) & \text{if } z \in \mathcal{V}^{\mathrm{irr}} \text{ has neighbouring vertices } z_1, z_2. \end{cases} \tag{2.3}$$

Its approximation properties are discussed in Lemma B.1 in §B of the appendix.

The Adini space V_h over $\mathcal{T}$ is assumed to be a subspace of $\widehat{V}_h$ from §2. This fixes the point values in all vertices, the gradient values in regular vertices, and, for any irregular vertex z, the partial derivative in tangential direction of the edge E containing z. It does not fix the partial derivative at z in the direction normal to E. We will new discuss possible choices in the next section.

3. Continuity conditions at hanging nodes

For an 1-irregular partition $\mathcal{T}$, an interior edge with a hanging node $z \in \mathcal{V}^{\mathrm{irr}}$ will be shared by three rectangles: one rectangle T for which z is not a vertex, $z \notin \mathcal{V}(T)$, and two rectangles K_1, K_2 which have z as a vertex, see Figure 3. The local degrees of freedom related to z cannot be a global degree of freedom. Instead, a choice for the value of the function and its gradient at z has to be made. For global continuity, it is necessary that v and the tangential derivative of v are continuous at z. The only freedom that is left is the choice of the derivative normal to T at z. Any sensible choice must guarantee approximation and consistency. We ask the assignment of the normal derivative to be linear, local, and invariant under relabelling of coordinates:

Definition 3.1 (admissible assignment)**.** Let $z \in \mathcal{V}^{\mathrm{irr}}$ be an irregular vertex. There exist exactly three elements $T, K_1, K_2 \in \mathcal{T}$ that contain z, where z is a vertex of K_1, K_2 and belongs to the interior of an edge E of T (see Figure 3) with normal vector n_E. A function $v \in \widehat{V}_h$ is said to satisfy an admissible assignment at z if

$$\frac{\partial v|_{K_1}}{\partial n_E}(z) = \frac{\partial v|_{K_2}}{\partial n_E}(z) = L(v|_T)$$

for a linear operator L that (1) is invariant under rotations by $\pi/2$ or reflections of the coordinate system and linear scaling (homothety) and (2) conserves quadratic polynomials. A subspace $V_h \subseteq \widehat{V}_h$ is said to satisfy an admissible assignment if any $v_h \in V_h$ satisfies an admissible assignment at every $z \in \mathcal{V}^{\mathrm{irr}}$ and if the kernel of a_h over V_h equals $\{0\}$.

Throughout this work, we assume that V_h is a linear subspace of $\widehat{V}_h$ satisfying an admissible assignment; in particular a_h is a scalar product on V_h. Then problem

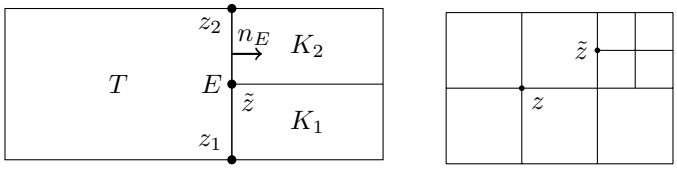

FIGURE 3. Left: Configuration with a hanging node $\tilde{z}$. Right: Mesh configuration with a regular vertex z and exactly one irregular vertex $\tilde{z}$ on $\partial\omega_z$.

(2.2) has a unique solution $u_h \in V_h$, and the classical a priori error bound [2, Lemma 10.1.7] known as Berger–Scott–Strang lemma states that

$$\max\{A, B\} \le \|\!|u - u_h|\!\|_h \le A + B \tag{3.1}$$

for the approximation and consistency errors

$$A := \inf_{v_h \in V_h} \|\!|u - v_h|\!\|_h \quad \text{and} \quad B := \sup_{v_h \in V_h \setminus \{0\}} a_h(u - u_h, v_h) \Big/ \|\!|v_h|\!\|_h.$$

For the method to converge at rate h^s it is necessary that both A and B decrease at least at that rate. A priori error estimates are usually formulated on sequences of uniformly refined meshes. Here, uniform refinement means that every rectangle is split into four equal sub-rectangles by connecting the midpoints of opposite edges with straight lines. If this refinement process is started from an initial 1-irregular partition, eventually the partition will contain regular vertices z with exactly one irregular vertex on the boundary of their vertex patch ω_z, as displayed Figure 3.

We say a method is $O(h^s)$ if there exists a constant $C > 0$ such that $\|\!|u - u_h|\!\|_h \le Ch^s(\|u\|_{H^4(\Omega)} + \|u\|_{W^{3,\infty}(\Omega)})$ provided the norm of u on the right-hand side is finite. According to the assignment rule of Definition 3.1, the space V_h is spanned by global basis functions related to the degrees of freedom at regular vertices. The following lemma states that necessary for convergence better than $O(h)$ is that the basis functions related to gradient evaluations are continued by 0 by the admissible assignment.

Lemma 3.2. *Let $\mathcal{T}$ be an 1-irregular partition such that there exists a regular vertex $z \in \mathcal{V}^{\mathrm{reg}}$ with exactly one irregular vertex $\tilde{z} \in \mathcal{V}^{\mathrm{irr}}$ on the boundary of its vertex patch (see Figure 3). Let $E \subseteq \partial\omega_z$ denote the edge containing $\tilde{z}$. Let $\varphi = \varphi_{z,\alpha}$ with $|\alpha| = 1$ denote the Adini basis functions with respect to the derivative evaluation at z (defined in §A of the appendix) with respect to the multiindex α. If $\partial_{n_E}\varphi_{z,\alpha}(\tilde{z})$ follows an admissible assignment and $\varphi_{z,\alpha}$ is not continued by 0 outside ω_z, then there exists an f such that the solution u belongs to $H^4(\Omega) \cap W^{3,\infty}(\Omega)$, but $\|\!|u - u_h|\!\|_h \ge c_1 h_E - c_2 h_E^2$ with positive numbers c_1, c_2 independent of the mesh size.*

Proof. Let u be the solution to (2.1) and assume $u \in H^4(\Omega)$. Consider the consistency term B from the a priori result (3.1). Due to (2.2) it satisfies

$$B \ge \|\!|\varphi|\!\|_h^{-1} \left(a_h(u, \varphi) - \int_\Omega f\varphi \right).$$

We follow the notation of Figure 3 and denote by K_1, K_2 the rectangles with $\tilde{z} \in \mathcal{V}(K_1) \cap \mathcal{V}(K_2)$. Clearly, due to the locality in Definition 3.1, φ vanishes identically outside $\omega_z \cup K_1 \cup K_2$, and we have with some real number c that

$$\varphi|_{K_1 \cup K_2} = c\psi$$

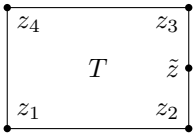

FIGURE 4. Notation for the reference rectangle used in Lemma 3.3.

where ψ is the (local) basis function with $\psi = \varphi_{\tilde{z},\beta}$ on $K_1 \cup K_2$ with $\beta \neq 0$ parallel to n_E (see §A of the appendix for the notation around the Adini basis functions). From standard scaling we thus have

$$\|D_h^2\varphi\|_{L^2(K_1\cup K_2)} \approx |c| \quad \text{and} \quad \|D_h^2\varphi\|_{L^2(\omega_z)} \approx 1.$$

The scaling invariance of Definition 3.1 implies $|c| \approx 1$ so that

$$|\!|\!|\varphi|\!|\!|_h \approx 1.$$

Thus,

$$B \gtrsim \left(\int_{\omega_z \cup K_1 \cup K_2} D^2 u : D^2\varphi - \int_\Omega f\varphi \right).$$

From scaling of φ we also have

$$\left| \int_\Omega f\varphi \right| \lesssim h_E^2 \|f\|_{L^2(\Omega)}.$$

Further, it can be computed (see Lemma A.4 in §A of the appendix) that

$$\int_{\omega_z} p\, \partial_{jk,h}^2 \varphi = 0 \quad \text{for any affine } p \in P_1 \text{ and any } j,k = 1,2.$$

Standard estimates thus show that $\int_{\omega_z} D^2 u : D^2\varphi$ is bounded by a constant times $h_E^2 \|u\|_{H^4(\Omega)}$. We thus obtain constants C_1, C_2 such that

$$B \geq -C_1 h_E^2 (\|u\|_{H^4(\Omega)} + \|f\|_{L^2(\Omega)}) + C_2 \int_{K_1\cup K_2} D^2 u : D_h^2 \varphi.$$

Now, by the above requirements, $\varphi|_{K_1\cup K_2}$ must coincide with $c\psi$. We explicitly compute with Lemma A.5 that

$$\int_{K_1\cup K_2} D_h^2 \varphi = c\, h_E \begin{bmatrix} \gamma_1 & 0 \\ 0 & \gamma_2 \end{bmatrix} \quad \text{with } \gamma_1\gamma_2 = 0 \text{ and } \gamma_1 + \gamma_2 \neq 0.$$

Without loss of generality, assume that $\gamma_1 > 0$. Then, if $D^2 u$ is uniformly positive definite in a neighbourhood of $K_1 \cup K_2$, we get the asserted lower bound for B. Such u can be easily obtained by multiplying the function $x^2 + y^2$ with a smooth cutoff function. □

The foregoing Lemma 3.2 has the following implication. The lower bound in the proof is better than linear only if $c = 0$. If $\partial_{n_E}\varphi_{z,\alpha}(\tilde{z})$ follows an admissible assignment and the method convergence like $O(h^s)$ with $s > 1$ on quasi-uniform meshes, then necessarily $\varphi_{z,\alpha}$ is continued by 0 outside ω_z. For the assignment operator L, using the notation for reference element displayed in Figure 4 with hanging node z, the lemma states that L must map the basis functions $\varphi_{z_1,\alpha}$ and $\varphi_{z_4,\alpha}$ with $|\alpha| = 1$ to zero. The next result shows that the averaging is the only potentially superlinear admissible refinement rule that preserves quadratic polynomials. Recall the Adini basis functions from §A of the appendix.

Lemma 3.3. *Consider the reference square $(-1,1)^2$ from Figure 4. with vertices $z_1,\dots,z_4$ in counterclockwise enumeration starting with $z_1=(-1,-1)$. Further denote $\tilde{z}=(1,0)$. The only linear admissible (in the sense of Definition 3.1) map $L:\mathcal{A}\to\mathbb{R}$ with*

$$L\varphi_{z_j,\beta}=0 \text{ for } j=1,4 \text{ and } |\beta|=1 \quad \text{and} \quad \partial_x p(\tilde{z})=Lp \quad \text{for all } p\in P_2$$

is the averaging

$$Lp:=\frac{1}{2}(\partial_x p(z_2)+\partial_x p(z_3)).$$

The space P_3 of cubic polynomials is not invariant under such assignment.

Proof. Since $P_3\subseteq\mathcal{A}$, any cubic polynomial can be represented in the Adini basis as

$$p=\sum_{j=1}^{4}\sum_{|\alpha|\le 1}\partial^\alpha p(z_j)\varphi_{j,\alpha}.$$

From linearity of L and the assumptions, we obtain

$$Lp=\sum_{j=1}^{4}p(z_j)L\varphi_{j,(0,0)}+\sum_{j=2,3}\sum_{|\alpha|=1}\partial^\alpha p(z_j)L\varphi_{j,\alpha}.$$

The quadratic polynomial $q=(x-1)^2/4$ then satisfies

$$Lq=\sum_{j=1,4}q(z_j)L\varphi_{j,(0,0)}$$

so that necessary for $\partial_x q(\tilde{z})=Lp$ is $L\varphi_{1,(0,0)}+L\varphi_{4,(0,0)}=0$ and thus $L\varphi_{1,(0,0)}=L\varphi_{4,(0,0)}=0$ from the coordinate-invariance. The quadratic polynomial $q=(y^2-1)/2$ then satisfies

$$Lq=\sum_{j=2,3}L\varphi_{j,(0,1)}$$

and, as above, this leads to $L\varphi_{z_2,(0,1)}=L\varphi_{z_3,(0,1)}=0$. Plugging in the polynomial $q=y^2$ then yields with an analogous argument that $L\varphi_{2,(0,0)}=L\varphi_{3,(0,0)}=0$. In summary, we obtain the necessary condition

$$Lp=\partial^{(1,0)}p(z_2)L\varphi_{z_2,(1,0)}+\partial^{(1,0)}p(z_3)L\varphi_{z_3,(1,0)}.$$

Obviously, the only choice that preserves quadratic polynomials (an their affine derivatives) over the edge containing $\tilde{z}$ is that $L\varphi_{z_2,(1,0)}=L\varphi_{z_3,(1,0)}=1/2$. It remains to check that this choice cannot preserve all cubic polynomials. For the choice $p=(1-y^2)(1-x)$, we see $\partial_x p$ vanishes at all vertices. Hence, we have $Lp=0$ but $\partial_x p(\tilde{z})=-1$. □

The foregoing two Lemmas 3.2–3.3 show that the averaging assignment is the only candidate that potentially achieves superlinear convergence, which in particular proves the lower error bound stated in Theorem A. Hence, the choice proposed here is to assign the average of the normal derivatives at the neighbouring vertices: The global Adini finite element spaces is defined by

$$V_h:=\left\{v\in\widehat{V}_h : Q\nabla v \text{ is continuous at } \mathcal{V}^{\mathrm{irr}}\right\}. \tag{3.2}$$

4. Analysis of the consistency error, Proof of Theorem A

Throughout this section, the choice of V_h is fixed through the averaging rule (3.2). On any T we introduce local coordinates

$$\xi(x,y) = h_x^{-1}(x-m) \quad \text{and} \quad \eta(x,y) = h_y^{-1}(y-m)$$

ranging from -1 to 1, where m is the midpoint of T and h_x, h_y are the half widths in x, y direction, respectively. By Q we denote the globally continuous and piecewise bilinear interpolation from (2.3). By the assignment of the hanging node value as in (3.2), the expression $Q\partial_x w$ is well defined for any $w \in V_h$. We note the following fact, which is essentially contained in [9].

Lemma 4.1. *Let T be a rectangle with E an edge orthogonal to the x-axis. Then any $w \in \mathcal{A}$ satisfies*

$$(1-Q)\partial_x w|_E = -\frac{h_y^3}{3}\partial^4_{xyyy} w(\eta^3-\eta) + \frac{h_y^2}{2}\partial^3_{xyy} w(\eta^2-1).$$

Proof. We express the monomials of the Adini space in terms of ξ, η. It is obvious that $\partial_x P_2$ and $\partial_x\langle \xi^2\eta, \eta^3\rangle$ belong to Q_1. Further $\partial_x\langle \xi^3, \xi^3\eta\rangle$ consists of functions that are linear in η and thus are interpolated exactly by Q on E. Therefore, the only two remaining monomials are $\xi\eta^2$, $\xi\eta^3$, and

$$(1-Q)\partial_x u|_E = (1-Q)\partial_x(a\xi\eta^3 + b\xi\eta^2)|_E$$

with real coefficients a, b. The chain rule reveals $\partial_x\xi = h_x^{-1}$, $\partial_y\eta = h_y^{-1}$. Taking derivatives of w and comparing coefficients shows that

$$\partial^4_{xyyy} w = \frac{6}{h_x h_y^3} a \quad \text{and} \quad \partial^3_{xyy} w = \frac{1}{h_x h_y^2}(6a\eta + 2b)$$

which leads to

$$a = \frac{h_x h_y^3}{6}\partial^4_{xyyy} w \qquad \text{and} \qquad b = \frac{h_x h_y^2}{2}\partial^3_{xyy} w - 3a\eta.$$

A direct computation of derivatives and interpolation leads to

$$(1-Q)\partial_x(a\xi\eta^3 + b\xi\eta^2) = h_x^{-1}\left(a(\eta^3-\eta) + b(\eta^2-1)\right).$$

Inserting the values for a and b in this formula reveals the asserted identity. □

The previous lemma will be essential for bounding the consistency term in the next lemma. We denote

$$\mathcal{T}^{\mathrm{reg}} := \{T \in \mathcal{T} : \text{all vertices of } T \text{ are regular}\} \qquad \text{and} \quad \mathcal{T}^{\mathrm{irr}} := \mathcal{T} \setminus \mathcal{T}^{\mathrm{reg}}. \tag{4.1}$$

Lemma 4.2. *Let the partition $\mathcal{T}$ satisfy the condition of Definition 2.1 and let V_h be chosen according to* (3.2)*. Let $g \in C^1(\Omega)$ be a piecewise polynomial function and $w \in V_h$. Then,*

$$\sum_{T\in\mathcal{T}} \int_{\partial T} g(1-Q)\nabla w \cdot n_T \lesssim (\|(1-\Pi_1)g\|_{\cup\mathcal{T}^{\mathrm{reg}}} + \|(1-\Pi_0)g\|_{\cup\mathcal{T}^{\mathrm{irr}}})\|D_h^2 w\|.$$

The constant hidden in the notation $\lesssim$ may depend on the polynomial degree of g.

Proof. We consider the edges orthogonal to the x or y axis separately. For a rectangle T we denote by n_x the x component of the outer unit normal (left -1, right 1, top and bottom 0). Fix any T with local coordinates (ξ, η). For $(1-Q)\partial_x w$ we use the expression from Lemma 4.1 and the fundamental theorem of calculus so that

$$\int_{\partial T} g(1-Q)\partial_x w n_x = -\frac{h_y^3}{3}\int_T \partial_x g\partial^4_{xyyy} w(\eta^3-\eta) + \frac{h_y^2}{2}\int_T \partial_x g\partial^3_{xyy} w(\eta^2-1). \tag{4.2}$$

Since the function $\eta^3-\eta$ has vanishing average over T, and since the fourth derivative of w is constant, we can use orthogonality to constants and the Cauchy inequality for the first term on the right-hand side of (4.2) to see

$$-\frac{h_y^3}{3}\int_T \partial_x g\partial^4_{xyyy}w(\eta^3-\eta) \le \frac{h_y^3}{3}\|(1-\Pi_0)\partial_x g\|_T\|\partial^4_{xyyy}w\|_T\|\eta^3-\eta\|_{L^\infty(\Omega)}. \tag{4.3a}$$

With the inverse estimate and $0\le\eta\le 1$ we obtain that this is bounded by some constant times

$$h_y\|(1-\Pi_0)\partial_x g\|_T\|\partial^2_{xy}w\|_T. \tag{4.3b}$$

Next, consider the second term of (4.2). With the global bilinear interpolation Q from (2.3) we obtain with the abbreviation $e:=w-Qw$ (note that $\partial^3_{xyy}w$ and $\partial^3_{xyy}e$ coincide) and integration by parts with respect to y that

$$\frac{h_y^2}{2}\int_T \partial_x g(\eta^2-1)\partial^3_{xyy}w = -\frac{h_y^2}{2}\int_T \partial^2_{xy}g(\eta^2-1)\partial^2_{xy}e - h_y\int_T \partial_x g\eta\partial^2_{xy}e.$$

Again, with integration by parts with respect to x,

$$-h_y\int_T \partial_x g\eta\partial^2_{xy}e = h_y\int_T \partial^2_{xx}g\eta\partial_y e - h_y\int_{\partial T}\partial_x g\eta\partial_y e n_x.$$

Integrating by parts along any edge E parallel to the y axis with end points z_-, z_+ reveals

$$-h_y\int_E \partial_x g\eta\partial_y e = h_y\int_E \partial^2_{xy}g\eta e + \int_E \partial_x g e - h_y((\partial_x g e)(z_+)+(\partial_x g e)(z_-)).$$

Combining the three foregoing displayed identities yields

$$\begin{aligned}&\frac{h_y^2}{2}\int_T \partial_x g(\eta^2-1)\partial^3_{xyy}w\\ &\quad= -\frac{h_y^2}{2}\int_T \partial^2_{xy}g(\eta^2-1)\partial^2_{xy}e + h_y\int_T \partial^2_{xx}g\eta\partial_y e + h_y\int_{\partial T}\partial^2_{xy}g\eta e n_x + R(T)\end{aligned} \tag{4.4}$$

with

$$R(T) := \int_{\partial T}\partial_x g e n_x - \sum_{z\in\mathcal{V}(T)} h_y n_x(\partial_x g e)(z).$$

We note that the inverse inequality implies for any second-order derivative ∂^2_{jk} of the polynomial $g|_T$ that

$$\|\partial^2_{jk}g\|_T \lesssim h_T^{-1}\|(1-\Pi_0)\partial_j g\|_T.$$

The combination of (4.2)–(4.4) with this estimate, the bound $0\le\eta\le 1$, trace and inverse inequalities, and the approximation and stability properties of Q from Lemma B.1, lead to

$$\int_{\partial T} g(1-Q)\partial_x w n_x \lesssim h_T\|(1-\Pi_0)\partial_x g\|_T\|\partial^2_{xy}w\|_T + R(T).$$

Of course we have $h_T\|(1-\Pi_0)\partial_x g\|_T \lesssim \|(1-\Pi_1)g\|_T$ for the polynomial $g|_T$. Considering the sum over all T, since $\partial_x g$ and e are globally continuous, we have that

$$\sum_{T\in\mathcal{T}}\int_{\partial T}\partial_x g e n_x = 0.$$

We further note that $e(z)=0$ for every regular vertex z. Therefore,

$$\sum_{T\in\mathcal{T}} R(T) \lesssim \sum_{T\in\mathcal{T}}\sum_{z\in\mathcal{V}(T)\cap\mathcal{V}^{\mathrm{irr}}} |h_T(\partial_x g e)(z)|.$$

Given $z \in V(T) \cap \mathcal{V}^{\rm irr}$, trace and inverse estimates show

$$|h_y(\partial_x g e)(z)| \lesssim \|(1-\Pi_0)g\|_T \|D_h^2 e\|_T.$$

Combining the above estimates results in the asserted identity with n_T replaced by n_x. An analogous argument shows the same bound for n_T replaced by n_y, so that eventually the full assertion follows. □

Proof of Theorem A. The abstract a priori error estimate (3.1) shows that the error is bounded by $A + B$. We start by bounding A. Let $I_h u$ denote the standard Adini interpolation of u described in §D of the appendix. On any element $T \in \mathcal{T}^{\rm reg}$ with regular vertices, the standard interpolation bound shows $\|D_h^2(u - I_h u)\|_T \lesssim h_T^2 \|D^4 u\|_T$. If $T \in \mathcal{T}^{\rm irr}$ contains an irregular vertex, I_h preserves quadratic functions and therefore the standard interpolation bound shows $\|D_h^2(u - I_h u)\|_T \lesssim h_T \|D^3 u\|_T$. Altogether,

$$A^2 \le \|D_h^2(u - I_h u)\|^2_{\cup \mathcal{T}^{\rm reg}} + \|D_h^2(u - I_h u)\|^2_{\cup \mathcal{T}^{\rm irr}} \lesssim h^4 \|u\|^2_{H^4(\cup \mathcal{T}^{\rm reg})} + h^2 \|u\|^2_{H^3(\cup \mathcal{T}^{\rm irr})}.$$

Under uniform mesh refinement, the area covered by elements with irregular vertices scales like

$$\operatorname{meas}(\cup \mathcal{T}^{\rm irr}) \lesssim h.$$

The assumed L^∞ bound on the third derivatives thus shows

$$A^2 \lesssim h^4 \|u\|^2_{H^4(\cup \mathcal{T}^{\rm reg})} + h^3 \|u\|^2_{W^{3,\infty}(\cup \mathcal{T}^{\rm irr})}.$$

For bounding the term B, consider any $v_h \in V_h$ with $|\!|\!| v_h |\!|\!|_h = 1$. Then, the solution property of u_h, integration by parts, and $\Delta^2 u = f$ show

$$a(u - u_h, v_h) = \sum_{T \in \mathcal{T}} \int_{\partial T} \partial^2_{nn} u \nabla w \cdot n_T = \sum_{T \in \mathcal{T}} \int_{\partial T} \partial^2_{nn} u (1 - Q) \nabla w \cdot n_T$$

because $Q \nabla w$ is continuous. Let $\boldsymbol{g} := \mathcal{J} D^2 u \in [C^1(\overline{\Omega})]^{2\times 2}$ denote the (componentwise) BFS averaging of $D^2 u$ defined in §C. Adding and subtracting $\boldsymbol{g}$ in the above identity results in

$$a_h(u - u_h, v_h) = \sum_{T \in \mathcal{T}} \int_{\partial T} (\partial^2_{nn} u - \boldsymbol{g}_{nn})(1 - Q) \nabla w \cdot n_T + \sum_{T \in \mathcal{T}} \int_{\partial T} \boldsymbol{g}_{nn} (1 - Q) \nabla w \cdot n_T.$$

Trace inequalities and the approximation and discrete stability properties of Q and $\mathcal{J}$ from Lemma B.1 and Lemma C.1 bound the first sum on the right-hand side as follows

$$\sum_{T \in \mathcal{T}} \int_{\partial T} (\partial^2_{nn} u - \boldsymbol{g}_{nn})(1 - Q) \nabla w \cdot n_T \lesssim h^2 \|u\|_{H^4(\Omega)} |\!|\!| w |\!|\!|_h.$$

The second term in the above split is bounded with the help of Lemma 4.2. A piecewise use of Poincaré's inequality and Lemma C.1 then concludes the proof of the upper error bounds in Theorem A. The stated lower error bound follows from Lemmas 3.2–3.3.

5. A posteriori error estimate, Proof of Theorem B

We define the projection operator $\Pi^{\mathcal{T}}$ by

$$\Pi^{\mathcal{T}} v|_T := \begin{cases} \Pi_1 v|_T & \text{if } T \in \mathcal{T}^{\rm reg} \\ \Pi_0 v|_T & \text{if } T \in \mathcal{T}^{\rm irr}. \end{cases} \tag{5.1}$$

Any edge is equipped with a fixed normal vector n_E and tangential vector t_E. The jump across E is denoted by $[\cdot]_E$; for boundary edges, $[\cdot]_E$ denotes the trace.

For any $T \in \mathcal{T}$ define the local error estimator contribution by

$$\boldsymbol{\eta}^2(T) = h_T^4 \|f\|_T^2 + \sum_{j=1}^{3} \sum_{E \in \mathcal{E}(T)} \kappa_j^E h_T^{2j-3} \left\| \left[\frac{\partial^j u_h}{\partial n_E^j} \right]_E \right\|_E^2 + \|(1 - \Pi^{\mathcal{T}}) D^2 u_h\|_T^2 \tag{5.2a}$$

where $\mathcal{E}(T)$ is the set of edges of T and

$$\kappa_j^E = \begin{cases} 0 & \text{if } j \geq 2 \text{ and } E \subseteq \partial\Omega, \\ 1 & \text{otherwise} \end{cases}$$

is introduced for excluding boundary edges from the sums when second- and third-order normal derivatives of u_h are considered. Define the total error estimator

$$\boldsymbol{\eta} = \left(\sum_{T \in \mathcal{T}} \boldsymbol{\eta}^2(T) \right)^{1/2}. \tag{5.2b}$$

Proof of Theorem B. As in [3], the error is orthogonally split as follows

$$\|\!|u - u_h|\!|_h^2 = \left[\sup_{\varphi \in H_0^2(\Omega) \setminus \{0\}} \frac{a_h(u - u_h, \varphi)}{|\!|\!|\varphi|\!|\!|_h} \right]^2 + \min_{v \in H_0^2(\Omega)} |\!|\!|u_h - v|\!|\!|_h^2$$

Since the second term on the right-hand side is directly bounded by $\boldsymbol{\eta}^2$ after plugging in the BFS averaging $v = \mathcal{J}_0 u_h$ with zero boundary conditions from §C and using the bound from Lemma C.1 and inverse estimates, it remains to bound the first term. Let $\varphi \in H_0^2(\Omega)$ with $|\!|\!|\varphi|\!|\!|_h = 1$ and denote by $I_h \mathcal{J} \varphi$ its Adini quasi-interpolation from §D of the appendix and abbreviate $\hat{\varphi} := \varphi - I_h \mathcal{J} \varphi$. Equation 2.1 and the discrete solution property (2.1) yield

$$a_h(u - u_h, \varphi) = \int_\Omega f \hat{\varphi} - a_h(u_h, \hat{\varphi}).$$

The first term on the right-hand side is readily bounded by $\boldsymbol{\eta}$ through (D.1). For the analysis of the second term, consider its contribution on any element T. Two integrations by parts reveal

$$\int_T D^2 u_h : D^2 \hat{\varphi} = \int_{\partial T} \partial_{nn}^2 u_h \partial_n \hat{\varphi} + \int_{\partial T} \partial_{nt}^2 u_h \partial_t \hat{\varphi} - \int_{\partial T} (\operatorname{div} D^2 u_h) \cdot n \hat{\varphi}.$$

Summing over all elements and noting that $\hat{\varphi}$ and so $\partial_t \hat{\varphi}$ is continuous, we obtain

$$a_h(u_h, \hat{\varphi}) = \sum_{T \in \mathcal{T}} \int_{\partial T} \partial_{nn}^2 u_h \partial_n \hat{\varphi} + \sum_{E \in \mathcal{E}} \Big(\int_E [\partial_{nt}^2 u_h]_E \partial_t \hat{\varphi} - \int_E [\operatorname{div} D^2 u_h]_E \cdot n_E \hat{\varphi} \Big).$$

Standard estimates [12] with (D.1) bound the last two terms by $\boldsymbol{\eta}$. In particular, by $\hat{\varphi} = \partial_t \hat{\varphi} = 0$ on $\partial\Omega$ the boundary edges do not contribute to the sum. For the analysis of the first sum on the right-hand side, denote by $\boldsymbol{g} := \mathcal{J} D_h^2 u_h$ the component-wise BFS averaging of the piecewise Hessian from §C. We have with the continuity of $\boldsymbol{g}$, $\nabla \mathcal{J}_h \varphi$, and $Q \nabla I_h \mathcal{J} \varphi$ that

$$\sum_{T \in \mathcal{T}} \int_{\partial T} \partial_{nn}^2 u_h \partial_n \hat{\varphi} = \sum_{T \in \mathcal{T}} \left(\int_{\partial T} (\partial_{nn}^2 u_h - \boldsymbol{g}_{nn}) \partial_n \hat{\varphi} + \int_{\partial T} \boldsymbol{g}_{nn} (1 - Q) \nabla I_h \mathcal{J} \varphi \cdot n_T \right).$$

The trace and inverse inequalities and Lemma 4.2 show that this is bounded by a constant times

$$\sum_{j=1,2} (\|\partial_{jj}^2 u_h - g_{jj}\| + \|(1 - \Pi^{\mathcal{T}}) g_{jj}\|)$$

where we used (D.1) and $\|D_h^2 \varphi\| \lesssim 1$. Since, obviously,

$$\|(1 - \Pi^{\mathcal{T}}) g_{jj}\| \leq \|(1 - \Pi^{\mathcal{T}}) \partial_{jj}^2 u_h\| + \|g_{jj} - \partial_{jj}^2 u_h\|$$

we eventually have

$$\sum_{T\in\mathcal{T}}\int_{\partial T}\partial_{nn}^2 u_h\partial_n\hat{\varphi}\lesssim(\|D_h^2u_h-\boldsymbol{g}\|+\|(1-\Pi^{\mathcal{T}})D^2u_h\|).$$

The last term is part of (and thus bounded by) $\boldsymbol{\eta}$. The bound of the first term follows from Lemma C.1. This concludes the proof of reliability. The efficiency follows from known arguments [12, 3].

6. Numerical results

6.1. **Illustration of Theorem A on quasi-uniform meshes.** We start by numerically illustrating the upper and lower a priori error bounds in an elementary setting with the square $\Omega=(-1,1)^2$ and f such that the exact solution is given by the biquartic polynomial $u=-(x^4-2x^2+1)(y^4-2y^2+1)$. We consider a regular coarse initial partition consisting of four congruent squares, and sequences of meshes following two refinement variants. In the first variant (Variant I), the coarse mesh is uniformly refined once, and thereafter only one element containing the point $(0,0)$ is refinement, resulting in an irregular partition. From this third mesh on, again uniform refinements are performed. In the second variant (Variant II), five uniform refinements of the initial mesh are performed before the seventh mesh is generated by refining only one element containing $(0,0)$. After that, the refinements are again uniform.

Starting from the third mesh in the sequence, the partitions of Variant I are irregular. Theorem A predicts the error to decrease as $h^{3/2}$ for V_h as in (3.2) and not better than h for any other choice. Up to the seventh mesh, the partitions of Variant II are uniform, so that Theorem A states errors of the order h^2 on these regular partitions. After the local refinement, the partitions are irregular, and Theorem A predicts the error for V_h as in (3.2) to gradually deteriorate to $h^{3/2}$, while any other method must immediately deteriorate from $O(h^2)$ to $O(h)$.

Figure 5 displays the convergence history of the $|||\cdot|||_h$ error with respect to the squareroot of the number of degrees of freedom `ndof`, which for these quasi-uniform meshes is proportional to h. Two assignments are compared: the assignment (3.2), abbreviated by V_h in the legend, and the enforcement of strong continuity of the normal derivative in irregular vertices, abbreviated by 'hard'. The results are as expected: for Variant I, the 'hard' interpolation results in convergence $O(h)$, while the method (3.2) reaches the predicted $O(h^{3/2})$. For Variant II, as soon as a single element is refined and, thus, the partition becomes irregular, the 'hard' interpolation method deteriorates to $O(h)$.

6.2. **Approximation of a curvilinear domain.** As an example for local resolution of a curved boundary, consider Ω as the unit disk with $f=1$ and the exact solution given by $u(x,y)=2^{-6}(x^2+y^2-1)^2$ and discretization by the averaging assignment (3.2). For the domain approximation, we consider a partition of the square $(-1,1)^2$ where all degrees of freedom related to vertices outside Ω are set to zero. On a sequence of uniformly refined meshes this results in convergence of order $h^{1/2}$ as can be seen in the convergence history of Figure 5. In a locally refined variant, from the j-th uniform refinement of the background mesh, the actual partition is generated by repeating j times: mark all elements that touch the boundary $\partial\Omega$ for local refinement and generate the smallest 1-irregular partition where the marked elements are refined. Figure 6 shows an instance of such a mesh; and the convergence history showing that this local refinement variant improves the convergence order to h.

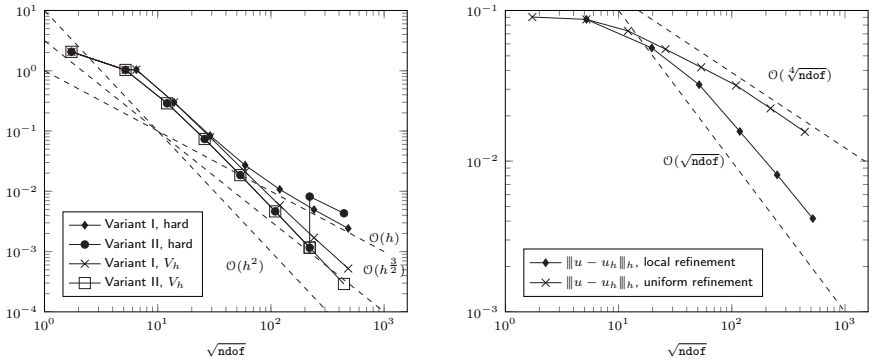

FIGURE 5. Right: Numerical illustration of Theorem A with the errors $|||u-u_h|||_h$ for a smooth u on the unit square, setting of §6.1. Left: Convergence history for the disk domain from §6.2.

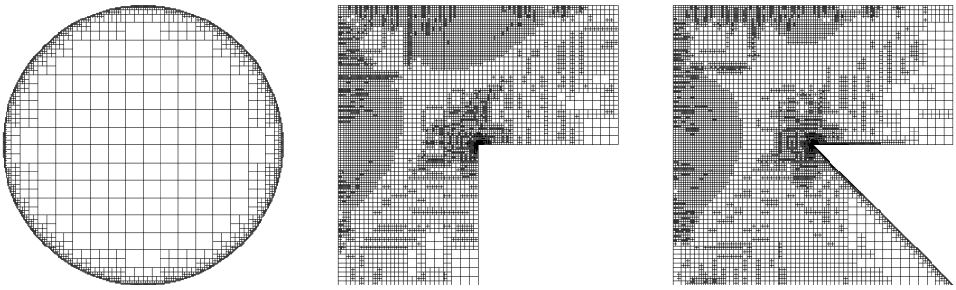

FIGURE 6. Left: Locally resolved disk, 13 875 degrees of freedom. Middle: Adaptive mesh of the L-domain, 36 798 degrees of freedom, level 17. Right: Adaptive mesh of the cusp domain, 44 793 degrees of freedom, level 20.

6.3. **Adaptive mesh refinement.** In this experiment, we consider the error estimator $\boldsymbol{\eta}$ with its local contributions $\boldsymbol{\eta}(T)$ as a refinement indicator in an adaptive mesh-refinement algorithm with Dörfler marking and bulk parameter chosen as 1/2 in a standard adaptivity loop [12]. We consider the L-shaped domain $\Omega = (-1,1)^2 \setminus ([0,1] \times [-1,0])$. With $\alpha = 0.5444837\ldots$ and $\omega = 3\pi/2$, the exact singular solution from [7, p. 107] reads in polar coordinates as

$$u(r,\theta) = (r^2\cos^2\theta - 1)^2(r^2\sin^2\theta - 1)^2 r^{1+\alpha} g(\theta), \tag{6.1}$$

with the function

$$g(\theta) = \left(\frac{s_-(\omega)}{\alpha-1} - \frac{s_+(\omega)}{\alpha+1}\right)(c_-(\theta) - c_+(\theta)) - \left(\frac{s_-(\theta)}{\alpha-1} - \frac{s_+(\theta)}{\alpha+1}\right)(c_-(\omega) - c_+(\omega)).$$

and the abbreviations $s_\pm(z) = \sin((\alpha \pm 1)z)$ and $c_\pm(z) = \cos((\alpha \pm 1)z)$. The convergence history with respect to the squareroot of the number of degrees of freedom (`ndof`) is displayed in Figure 7. As expected, uniform mesh refinement converges with the suboptimal rate dictated by α. Adaptive mesh refinement with the averaging assignment (3.2) recovers first-order convergence, while the variant enforcing the 'hard' interpolation constraint performs poorly (on the same adaptive meshes) because its error is bounded from below by certain elements of large mesh size (Theorem A), see the adaptive mesh displayed in Figure 6.

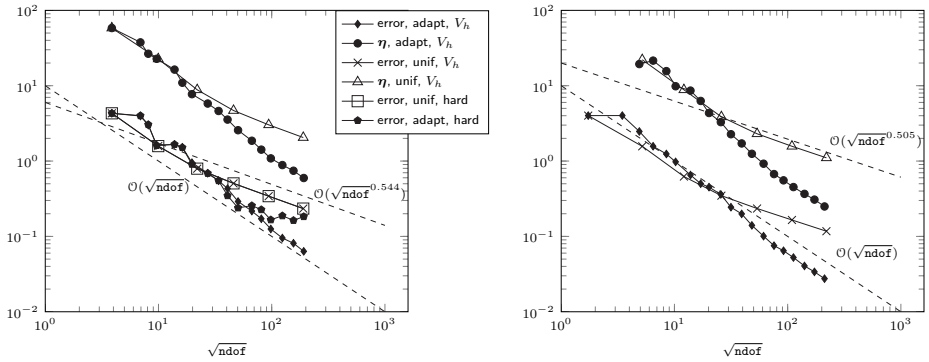

FIGURE 7. Convergence history for the of the error $|||u-u_h|||_h$ and the estimator $\boldsymbol{\eta}$ for the L-shaped (left) and the cusp (right) domain from §§6.3–6.4.

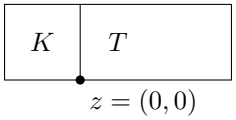

FIGURE 8. Vertex $z=(0,0)$ shared by T, K with common edge lying on the y axis.

6.4. **Approximation of a non-rectilinear domain.** As an example for adaptive resolution of a non-rectilinear domain, consider the corner domain $\Omega=(-1,1)^2\setminus \operatorname{conv}\{(0,0),(1,-1),(1,0)\}$ with exact solution given by (6.1) for the parameters $\alpha=0.50500969\ldots$ and $\omega=7\pi/4$. The line with angle $7\pi/4$ describes the non-rectilinear part of the boundary. We use an interior approximation with rectangles and add on elements T touching the boundary the local error estimator contribution $h_T^2\boldsymbol{\eta}^2$ to $\eta^2(T)$ in the marking process. This accounts for the error by the boundary approximation. Figure 7 shows the convergence history. As in the previous example, adaptive mesh refinement improves the reduced convergence observed on uniform meshes. An adaptive mesh is displayed in Figure 6.

APPENDIX A. PROPERTIES OF THE ADINI BASIS FUNCTIONS

The Adini basis function $\varphi_{z,\alpha}\in\widehat{V}_h$ with respect to a regular vertex $z\in\mathcal{V}^{\mathrm{reg}}$ and a multiindex $\alpha\in\{(0,0),(1,0),(0,1)\}$ satisfies

$$\partial^\beta\varphi_{z,\alpha}(\tilde z)=\delta_{z,\tilde z}\,\delta_{\alpha,\beta}\quad\text{for all }\tilde z\in\mathcal{V}^{\mathrm{reg}}\text{ and }\beta\in\{(0,0),(1,0),(0,1)\}$$

with the Kronecker δ. This uniquely defines $\varphi_{z,\alpha}$ on regular partitions. On partitions with irregular vertices, it uniquely defines $\varphi_{z,\alpha}$ on elements T with $\mathcal{V}(T)\subseteq\mathcal{V}^{\mathrm{reg}}$, that is, on elements with only regular vertices.

In what follows we consider two rectangles T, K sharing an edge lying on the y axis, with one vertex being $z=(0,0)$, as shown in Figure 8. The ratio of the x-widths of T, K is denoted by

$$\rho=\operatorname{diam}_x(T)/\operatorname{diam}_x(K).$$

The following results are formulated in the coordinates (x,y) if T,K are considered. If only T is considered, the usual local coordinates ξ,η are employed.

Lemma A.1. *In the configuration of Figure 8, $\varphi = \varphi_{z,(0,0)}$ satisfies*

$$\text{(a)} \int_T q\,\partial^2_{xx}\varphi = 0, \quad \text{(b)} \int_{T\cup K} x\,\partial^2_{xx}\varphi = 0, \quad \text{(c)} \int_{T\cup K} q\,\partial^2_{xy}\varphi = 0$$

for any integrable function $q = q(y)$ depending only on y.

Proof. For the proof of (a), we use local coordinates ξ, η, write $\hat{q}(\eta) = q(y)$, and observe that φ vanishes identically at $\eta = 1$ and $\partial^2_{xx}\varphi$ is bilinear, so that there exists a first-order polynomial $p_1 = p_1(\xi)$ such that $\partial^2_{xx}\varphi = (1-\eta)p_1(\xi)$. Since $\partial_x\varphi$ vanishes at all vertices of T, considering $\eta = -1$ with the fundamental theorem of calculus shows that

$$\int_{-1}^{1} \partial^2_{xx} p_1(\xi)\,d\xi = 0.$$

The original integral then reads

$$\int_T \hat{q}(\eta)\partial^2_{xx}\varphi = h_x h_y \int_{-1}^{1} \hat{q}(\eta)(1-\eta)\,d\eta \int_{-1}^{1} \partial^2_{xx} p_1(\xi)\,d\xi = 0.$$

For the proof of (b), we use the symmetry $\varphi|_K(x,y) = \varphi|_T(-\rho x, y)$ for $x \in K$. By the change of variables $\hat{x} = -\rho x$ we have for the (undirected) volume integrals that

$$\int_K x\partial^2_{xx}\varphi(x,y)\,dxdy = \int_T \frac{-\hat{x}}{\rho}\partial^2_{xx}\varphi(\hat{x},y)|-\rho^{-1}|\,d\hat{x}dy = -\int_T \hat{x}\partial^2_{\hat{x}\hat{x}}\varphi(\hat{x},y)\,d\hat{x}dy.$$

This implies (b). An analogous computation shows (c). □

Lemma A.2. *In the configuration of Figure 8, $\varphi = \varphi_{z,(1,0)}$ satisfies*

$$\text{(a)} \int_T x\,\partial^2_{xx}\varphi = 0, \quad \text{(b)} \int_T q\,\partial^2_{xy}\varphi = 0, \quad \text{(c)} \int_{T\cup K} q\,\partial^2_{xx}\varphi = 0.$$

for any integrable function $q = q(y)$ depending only on y.

Proof. Since φ vanishes on all sides apart from $\{\eta = -1\}$, it contains the linear factors $(\eta-1)(\xi+1)(\xi-1)$. Since $\varphi|_T \in \mathcal{A}$, for $\partial_x\varphi$ to vanish on the two endpoints of the face $\xi = 1$, an additional factor $(\xi - 1)$ is necessary. The presence of the resulting factor $(\xi-1)^2$ shows that φ_x vanishes on the whole face $\xi = 1$. Integration by parts then reads

$$\int_T x\partial^2_{xx}\varphi = -\int_T \partial_x\varphi.$$

This equals zero because φ has zero boundary conditions, which proves (a). For the proof of (b), integration by parts with respect to y shows

$$h_y \int_T \hat{q}(\eta)\partial^2_{xy}\varphi = h_y \sum_{\sigma=\pm 1} \int_{\{\eta=\sigma\}} \hat{q}(\sigma)\partial_x\varphi - \int_T \partial_y\hat{q}(\eta)\partial_x\varphi.$$

Integration by parts with respect to x shows that all these integrals vanish because φ vanishes identically on the edges parallel to the y axis. This shows (b). We note the symmetry $\varphi|_K(x,y) = -\rho^{-1}\varphi|_T(-\rho x, y)$. A computation analogous to that of the proof of (b) in Lemma A.1 thus proves (c). □

Lemma A.3. *In the configuration of Figure 8, $\varphi = \varphi_{z,(0,1)}$ satisfies*

$$\int_{T\cup K} q\,\partial^2_{xy}\varphi = 0 \quad \textit{and} \quad \partial^2_{xx}\varphi = 0$$

for any integrable function $q = q(y)$ depending only on y.

Proof. With the symmetry $\varphi|_K(x,y) = \varphi|_T(-\rho x, y)$, an argument similar to that of the proof of (b) in Lemma A.1 proves the first identity. Since the bilinear function $\partial^2_{xx}\varphi$ vanishes on the faces parallel to the x axis, we have $\partial^2_{xx}\varphi = 0$, which is the second asserted identity. □

Lemma A.4. *Let z be a regular interior vertex with patch ω_z. Any*

$$\varphi \in \{\varphi_{z,(0,0)}, \varphi_{z,(1,0)}, \varphi_{z,(0,1)}\}$$

out of the three global Adini basis functions related to z satisfies

$$\int_{\omega_z} p\,\partial^2_{jk}\varphi\,dx = 0 \quad \text{for any } p \in P_1 \text{ and any pair } (j,k) \in \{1,2\}^2.$$

Proof. This follows from carefully combining the foregoing three lemmas with suitable changes of coordinates. □

Lemma A.5. *In the configuration of Figure 8, $\varphi = \varphi_{z,(0,1)}$ satisfies*

$$\int_{T\cup K} D^2\varphi = h_T \begin{bmatrix} 0 & 0 \\ 0 & \gamma \end{bmatrix} \quad \text{with } \gamma \approx 1.$$

Proof. Lemma A.3 shows that $\int_{T\cup K} \partial^2_{jk}\varphi = 0$ if $\min\{j,k\} \le 1$. From the symmetry $\varphi|_K(x,y) = \varphi|_T(-\rho x, y)$ and change of variables we further obtain

$$\int_K \partial^2_{yy}\varphi = \rho^{-1}\int_T \partial^2_{yy}\varphi \qquad \text{and therefore} \quad \int_{T\cup K} \partial^2_{yy}\varphi = (1+\rho^{-1})\int_T \partial^2_{yy}\varphi.$$

Since φ vanishes on all edges of T apart from $\{\xi = -1\}$, an argument analogous to that of the proof of Lemma A.2 shows that $\varphi = c(\eta-1)^2(\eta+1)(\xi-1)$ with some $c \approx h_y$. Then, obviously, the integral of $\partial^2_{yy}\varphi = h_y^{-2}c(\xi-1)(6\eta+2)$ over T is nonzero and scales like h_T. □

Appendix B. Bilinear interpolation with hanging-node constraint

B.1. **Bilinear interpolation.** Given a piecewise polynomial function w that is continuous in the regular vertices of $\mathcal{T}$, its globally continuous and piecewise bilinear interpolation Qw is defined in (2.3).

Lemma B.1 (stability and approximation of bilinear interpolation)**.** *Let the 1-irregular partition $\mathcal{T}$ satisfy the mesh condition of Definition 2.1 and let the function w be globally continuous and piecewise polynomial with respect to $\mathcal{T}$. Then*

$$h_T^{-2}\|w - Qw\|_T + h_T^{-1}\|\nabla(w-Qw)\|_T + \|D^2 Qw\|_T \lesssim \|D^2_h w\|_{\omega_T} \quad \text{for any } T \in \mathcal{T},$$

with the element patch ω_T. The constant hidden in the notation $\lesssim$ depends on the polynomial degree of w.

Proof. If T exclusively has regular vertices, Q is the standard bilinear interpolation on T and the result is obvious. Assume therefore that T has an irregular vertex z. Then z belongs to an edge with two neighbouring regular vertices one of them lying outside T. By the mesh condition, T must possess at least two regular vertices, so that in total there are at least three regular vertices inside $\overline{\omega}_T$. At these points $w = Qw$ holds. The asserted result thus follows from a standard scaling argument and the finite number of possible local mesh configurations. □

Appendix C. BFS averaging

It is well known from the Bogner–Fox–Schmid (BFS) finite element [5] that, on any rectangle, the 16 linear functionals

$$v \mapsto \partial^\alpha v(z) \quad \text{for any vertex } z \text{ of } T \text{ and any } \alpha \in \mathfrak{B}$$

for the set $\mathfrak{B} := \{(0,0),(1,0),(0,1),(1,1)\}$ of multiindices are linear independent over Q_3 (bicubic functions). The corresponding dual BFS basis of Q_3 consists of the 16 functions $\psi_{z,\alpha}$ with

$$\partial^\beta \psi_{z,\alpha}(\tilde{z}) = \delta_{z,\tilde{z}}\delta_{\alpha,\beta} \quad \text{for all } z,\tilde{z} \in \mathcal{V}(T) \text{ and } \alpha,\beta \in \mathfrak{B}.$$

As a basic averaging operator, introduce $\mathcal{M}$ and $\mathcal{M}_0$ mapping a piecewise smooth function v to a piecewise Q_3 function by assigning the mean of the above local functionals at *all vertices* (resp. all interior vertices). More precisely, for every rectangle $T \in \mathcal{T}$ and any vertex $z \in \mathcal{V}(T)$ of T, they are defined by

$$(\partial^\alpha \mathcal{M} v|_T)(z) := \overline{\sum_{\substack{K\in\mathcal{T}:\\ z\in K}} (\partial^\alpha v|_K)(z)} \qquad \text{and} \qquad (\partial^\alpha \mathcal{M}_0 v|_T)(z) := \begin{cases} \mathcal{M}(z) & \text{if } z \in \Omega \\ 0 & \text{if } z \in \partial\Omega \end{cases}$$

(the Σ with the bar represents the average). This function is C^1 continuous in all regular vertices, but it may be discontinuous at irregular vertices. From $\mathcal{M}v$ (resp. $\mathcal{M}_0 v$) we construct a globally C^1 and piecewise bicubic (thus BFS) function $\mathcal{J}v$ (resp. $\mathcal{J}_0 v$) by assigning the values of $\mathcal{M}v$ (resp. $\mathcal{M}_0 v$) at regular vertices and by matching the values at irregular vertices by interpolation, more precisely

$$(\partial^\alpha \mathcal{J} v)(z) = \begin{cases} (\partial^\alpha \mathcal{M} v)(z) & \text{if } z \in \mathcal{V}^{\mathrm{reg}} \\ (\partial^\alpha \mathcal{M} v|_T)(z) & \text{if } z \in \mathcal{V}^{\mathrm{irr}} \text{ and } z \in T \setminus \mathcal{V}(T). \end{cases}$$

The definition of $\mathcal{J}_0$ is analogous with $\mathcal{M}$ replaced by $\mathcal{M}_0$ in the above formula. In the general case that v is piecewise H^2-regular, we overload notation and extend $\mathcal{J}$ by defining $\mathcal{J}v := \mathcal{J}\Pi_{Q_3} v$ for the L^2 projection Π_{Q_3} to piecewise bicubic functions. As in prior sections we denote by $[\cdot]_E$ the jump across an edge E.

Lemma C.1. *Let $\mathcal{T}$ be an 1-irregular partition satisfying the mesh condition of Definition 2.1. Any piecewise Q_3 (bicubic) function $v \in L^2(\Omega)$ satisfies*

$$\|v - \mathcal{J}_0 v\|^2 \lesssim \sum_{E\in\mathcal{E}} \left(h_E \|[v]_E\|_E^2 + h_E^3 \|[\nabla v]_E\|_E^2 \right).$$

If $v \in H^2(\Omega)$, we have

$$\|h^{-2}(v - \mathcal{J}v)\| + \|h^{-1}\nabla(v - \mathcal{J}v)\| + \|D^2 \mathcal{J} v\| \lesssim \|D^2 v\|.$$

Proof. Let v be piecewise bicubic. Let $T \in \mathcal{T}$ and $z \in \mathcal{V}(T)$ be a vertex of T. Standard techniques [2, 3] reveal for the basic averaging operator $\mathcal{M}_0$ that

$$\sum_{\alpha\in\mathfrak{B}} h_T^{1+|\alpha|} |\partial^\alpha (v - \mathcal{M}_0 v)(z)| \lesssim \left(\sum_{E\in\mathcal{E}: z\in E} (h_T \|[v]_E\|_E^2 + h_T^3 \|[\nabla v]_E \cdot n_E\|_E^2) \right)^{1/2}.$$

If z is a regular vertex, the same estimate obviously holds for $\mathcal{M}_0$ replaced by $\mathcal{J}_0$. If z is an irregular vertex and K is the element with $z \in K \setminus \mathcal{V}(K)$, then $(\partial^\alpha \mathcal{J}_0 v)(z)$ is defined by interpolation from information of $\mathcal{M}_0 v$ in the neighbouring vertices z_1, z_2; and a scaling argument shows that

$$(\partial^\alpha (v - \mathcal{J}_0 v)|_T)(z) = (\partial^\alpha v|_T - \partial^\alpha \mathcal{M}_0 v|_K)(z) \lesssim \sum_{j=1}^{2} \sum_{\beta\in\mathfrak{B}} h_T^{|\beta|-|\alpha|} \left| \partial^\beta (v - \mathcal{M}_0 v)|_{T_j}(z_j) \right|$$

where T_1, T_2 are the two rectangles with $\{z, z_j\} \subseteq \mathcal{V}(T_j)$ (one of them being T). Since the expansion of $v - \mathcal{J}_0 v$ on T in terms of the BFS basis functions and the scaling of the latter read

$$(v - \mathcal{J}_0 v)|_T = \sum_{\alpha\in\mathfrak{B}} \sum_{z\in\mathcal{V}(T)} \partial^\alpha (v - \mathcal{J}_0 v)(z) \psi_{\alpha,z} \qquad \text{and} \qquad \|\psi_{\alpha,z}\|_T \lesssim h_T^{1+|\alpha|},$$

a direct computation with the triangle inequality and the above estimates at the vertices and the local equivalence $h_T \approx h_E$ reveal that

$$\|v - \mathcal{J}_0 v\|_T = \left(\sum_{z\in\mathcal{V}(T)} \sum_{E\in\mathcal{E}: z\in E} (h_E \|[v]_E\|_E^2 + h_E^3 \|[\nabla v]_E \cdot n_E\|_E^2) \right)^{1/2}.$$

This and the finite overlap of the element patches proves the first stated estimate for $\mathcal{J}_0$. An analogous argument shows that the same upper bound is valid for $\|v - \mathcal{J}v\|^2$. The second stated estimate follows from combining this bound with local trace inequalities and standard estimates for the piecewise L^2 projection. □

We remark that in the upper bound of $\|v - \mathcal{J}v\|^2$ mentioned in the proof of the foregoing lemma, the boundary edges can be dropped, which is, however, not made use of in this work.

Appendix D. Adini quasi-interpolation

We denote by I_h the standard Adini interpolation with zero boundary data acting an a sufficiently smooth function w as

$$I_h w|_T = \sum_{z\in\mathcal{V}(T)\cap\Omega} \sum_{|\alpha|\leq 1} \partial^\alpha w(z)\varphi_{z,\alpha} \quad \text{for any } T \in \mathcal{T}$$

with $\varphi_{z,\alpha}$ defined in §A. Let $v \in H^2_0(\Omega)$. We define the Adini quasi-interpolation $I_h\mathcal{J}v \in V_h$, where $\mathcal{J}$ is the BFS averaging from §C. With Lemma C.1 and standard discrete estimates we obtain

$$\|h^{-2}(v - I_h\mathcal{J}v)\| + \|h^{-1}\nabla(v - I_h\mathcal{J}v)\| + \|D^2_h I_h\mathcal{J}v\| \lesssim \|D^2 v\|. \tag{D.1}$$

References

[1] A. Adini and R. W. Clough. Analysis of plate bending by the finite element method. *NSF report*, G-7337, 1961.

[2] S. C. Brenner and L. R. Scott. *The Mathematical Theory of Finite Element Methods*, volume 15 of *Texts in Applied Mathematics*. Springer, New York, third edition, 2008.

[3] C. Carstensen, D. Gallistl, and J. Hu. A posteriori error estimates for nonconforming finite element methods for fourth-order problems on rectangles. *Numer. Math.*, 124(2):309–335, 2013.

[4] C. Carstensen and J. Hu. Hanging nodes in the unifying theory of a posteriori finite element error control. *J. Comput. Math.*, 27(2-3):215–236, 2009.

[5] P. G. Ciarlet. *The Finite Element Method for Elliptic Problems*, volume 4 of *Studies in Mathematics and its Applications*. North-Holland, Amsterdam, 1978.

[6] D. Gallistl and S. Tian. A posteriori error estimates for nonconforming discretizations of singularly perturbed biharmonic operators. *SMAI J. Comput. Math.*, 10:355–372, 2024.

[7] P. Grisvard. *Singularities in Boundary Value Problems*, volume 22 of *Recherches en Mathématiques Appliquées*. Masson, Paris, 1992.

[8] T. Gudi. A new error analysis for discontinuous finite element methods for linear elliptic problems. *Math. Comp.*, 79(272):2169–2189, 2010.

[9] J. Hu, X. Yang, and S. Zhang. Capacity of the Adini element for biharmonic equations. *J. Sci. Comput.*, 69(3):1366–1383, 2016.

[10] P. Lascaux and P. Lesaint. Some nonconforming finite elements for the plate bending problem. *Rev. Française Automat. Informat. Recherche Operationnelle*, 9(R-1):9–53, 1975.

[11] E. Oñate. *Structural analysis with the finite element method—linear statics. Volume 1. Basis and solids*. Lecture Notes on Numerical Methods in Engineering and Sciences. International Center for Numerical Methods in Engineering (CIMNE), Barcelona; Springer-Verlag, Berlin, 2009.

[12] R. Verfürth. *A posteriori error estimation techniques for finite element methods*. Numerical Mathematics and Scientific Computation. Oxford University Press, Oxford, 2013.

Institut für Mathematik, Universität Jena, 07743 Jena, Germany
Email address: dietmar.gallistl [at] uni-jena.de